

# Wideband Circulators for Use at Frequencies Above 100 GHz to Beyond 350 GHz

Derek H. Martin and Richard J. Wylde

**Abstract**—High-performance circulators operating at frequencies in the range from 100 to 350 GHz have been developed for application in major measurement systems. These circulators have open quasi-optical structures. The magnetized plates in these devices are of nonmetallic magnetic materials which have both well-developed millimeter-wave gyrotropic properties and the magneto-static properties of an excellent permanent magnet material. Very few commercially available magnetic materials have been found that meet both the magnetostatic and the magneto-optical selection criteria. Those few have, however, made possible the design, manufacture, and successful operation of high-performance circulators/isolators at these high operating frequencies. Several circulators/isolators of this type have been installed in major measurement systems.

**Index Terms**—Millimeter-wave and submillimeter-wave circulators and isolators, quasi-optical circulators and isolators.

## I. INTRODUCTION

CIRCULATORS are serving important signal-controlling functions in many microwave and millimeter-wave measurement systems operating at frequencies below 100 GHz. We have developed high-performance circulators that can provide similar signal-controlling functions at frequencies above 100 GHz to beyond 350 GHz. These circulators have already been incorporated in a number of major millimeter/submillimeter-wave measurement systems and a wide use of such circulators can be expected in the future as measurement systems in this range of frequency continue to grow in number and importance.

To achieve high-level circulator performance above 100 GHz it is necessary to use open quasi-optical structures such as the four-port illustrated in Fig. 1. A free-space high-directivity signal beam that is incident in Port 1, with its linear-polarization transverse to the metallic wires of the grid in that port, will pass through the grid, through the Faraday-rotator plate (in which its polarization is turned through  $45^\circ$ ) and through the second grid, to emerge with little overall loss in Port 2. Generally, signal beams entering and leaving the ports of this structure do so according to the nonreciprocal circulator scheme  $1 \Rightarrow 2, 2 \Rightarrow 3, 3 \Rightarrow 4$ , and  $4 \Rightarrow 1$ . (The direction of linear-polarization defined for each port is determined by the

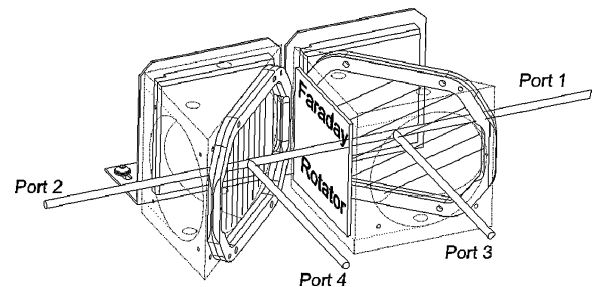


Fig. 1. Quasi-optical Faraday-rotation circulator. The Faraday-rotator plate at the center is of a nonmetallic magnetic material, fully magnetized normally to its surfaces, with surface layers of dielectric material to match a normally incident plane-polarized signal beam into the plate, and out of it following a single pass of the plate. The thickness of the plate is such that the signal beam suffers a  $45^\circ$  Faraday rotation of its plane of polarization in the single pass. This Faraday-rotator plate is located between two wire-grids set with their planes at  $45^\circ$  to the lines of the signal beams. The directions of the closely spaced wires in the two grids (as indicated here by a few lines drawn in the plane of each grid), when projected onto a transverse plane, are at  $45^\circ$  to each other. Planar power dumps are provided as indicated at the rear of the diagram. This circulator becomes an isolator if further power dumps are placed in Ports 3 and 4.

wire-grid in that port: for Ports 1 and 2, it is that for which the grid has near-unity transmittance, and for Ports 3 and 4, it is that for which the grid has near-unity reflectance. Any cross-polar component in an incident beam would go directly to a power dump.)

The magnetic material in the Faraday-rotator plate at the center of the circulator must clearly have well-developed gyrotropic properties at these high signal frequencies; in addition, it must have the magnetostatic characteristics of an excellent permanent magnet material. The latter requirement arises from the thin plate form of the Faraday rotator in a quasi-optical structure; this plate has to retain a high and uniform magnetization perpendicular to its surfaces in the presence of the very large demagnetizing field that acts inside a thin plate. (A surrounding magnet that would countervail this large demagnetizing field over the width of the plate without obtruding on the passage of the signal beam through the plate would be impracticably large and massive.) The use of a permanent magnet material was the enabling idea in our first-reported quasi-optical circulators [1], and in those recently described by colleagues [2], which operate at frequencies near 90 GHz. In this paper, we describe the development of high-performance circulators operating at higher frequencies, from 100 to 350 GHz and beyond, with particular attention to achieving the long-term operational stability necessary for application in major measurement systems.

Manuscript received June 30, 2008. First published December 22, 2008; current version published January 08, 2009.

D. H. Martin is with Queen Mary College, University of London, London E1 4NS, U.K. (e-mail: d.h.martin@qmul.ac.uk).

R. J. Wylde is with the School of Physics and Astronomy, University of St. Andrews, Fife KY16 9AL, U.K., and also with Thomas Keating Ltd, Billingshurst, West Sussex RH14 9SH, U.K. (e-mail: r.wylde@terahertz.co.uk).

Digital Object Identifier 10.1109/TMTT.2008.2008955

In this study, it has been necessary to formulate magneto-static and magneto-optical selection criteria for the magnetic materials to be used in the Faraday rotators (Sections II and III) and then to search for materials that meet these criteria. We have found very few commercially available materials that satisfy both the magnetostatic and the millimeter/submillimeter-wave magneto-optical criteria (Section IV). These few have, however, made possible the design, manufacture, and successful operation of a number of high-performance circulators operating in the range from 100 to 350 GHz, as described in Section VII.

In this study, it has also been necessary to make measurements of the magneto-optical constants of a large number of candidate materials over the range of 50–170 GHz, and for the few selected materials, up to 500 GHz. The method which, with colleagues, we have developed for this purpose is outlined in Section V. It has also been necessary to develop analytical procedures for calculating the properties of quasi-optical multilayer structures that incorporate gyrotropic materials in order to determine the design parameters of circulators and to predict reliably their performances. These procedures are described in Section VI.

## II. MAGNETOSTATIC PROPERTIES OF CANDIDATE MATERIALS

The thickness of the magnetized plate in a quasi-optical circulator is to be such as will give a  $45^\circ$  Faraday rotation in a single pass of the plate (typically one or two millimeters); the width of the plate is to be such as will accommodate a signal beam of moderately high directivity (a few tens of millimeters). The plate will thus be “thin,” and when fully magnetized perpendicularly to its surfaces it will be subject to an extremely high demagnetizing field,  $H_d = -M$ , where  $M$  is the magnetization in the plate. If the plate is to retain its near-homogeneous near-uniform, magnetization along its axis on removal from the large external magnet in which it is initially poled, the material of the plate must have the characteristics of an excellent permanent magnet material; that is to say: 1) the material must be uniaxially highly anisotropic magnetically; its demagnetization curve (the progressive reduction of the mean magnetization,  $M$ , from a near-saturation value to zero as a negative magnetic field acting inside the material,  $-H$ , increases in magnitude from zero up to the coercive field of the material) must be near-rectangular in form (see Fig. 2) and 2) the *operating point* of a thin plate of the material must be *above the knee* of the demagnetization curve. The operating point is the point on the material’s demagnetization curve to which the material in a thin plate will be taken by the demagnetizing field inside it; i.e., at the intersection of the line  $M = -H$  with the demagnetization curve (see Fig. 2).

The nonmetallic metal–oxide fine-grained ceramics, known as *hexaferrites*, which are produced commercially for the fabrication of permanent magnets for a host of static-field applications, are the candidate materials for first consideration. They are prepared in a range of chemical compositions, using a variety of forming processes, including treatments which produce a high degree of co-alignment of the grains’ hexagonal axes (within a range of a few degrees). Each grain exhibits a very large intrinsic uniaxial magneto-crystalline anisotropy which,

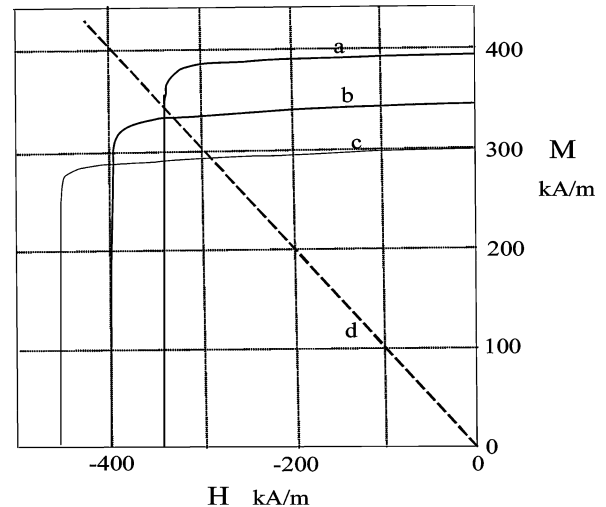


Fig. 2. Near-rectangular demagnetization curves of the FB9H hexaferrite ceramic from TDK,<sup>1</sup> at temperature: (a)  $-40^\circ\text{C}$ , (b)  $20^\circ\text{C}$ , and (c)  $100^\circ\text{C}$  (based on the supplier’s data sheets). The operating point for a thin plate of a material is at the intersection of the line  $M = -H$  (line d) with the demagnetization curve, which is above the knee for FB9H at  $20^\circ\text{C}$  and at  $100^\circ\text{C}$ , but below the knee at  $-40^\circ\text{C}$ .

given the preferred orientation of the grains, results in these materials satisfying requirement 1) above very well (see the examples in Fig. 2). Only a few of the commercially available hexaferrites, however, provide a sufficient ratio of coercive field to remanent-magnetization to satisfy requirement 2). Fig. 2 shows demagnetization curves for the hexaferrite FB9H supplied by TDK,<sup>1</sup> which is one of the few that do so.

The importance of requirement 2) above is that, in a grain-oriented material in a state above the knee of its demagnetization curve, the magnetization is close to being homogeneous and uniform since the direction of the spontaneous magnetization in each grain is within a few degrees of the material axis. The correlation length of the small random deviations from strict homogeneity will be no more than a few grain diameters, i.e., a few micrometers. A coherent millimeter/submillimeter-wave signal beam propagating through a material in this state might suffer some weak diffuse scattering at these small short-range deviations (appearing as a weak contribution to the attenuation of the beam), but will otherwise propagate as if the material were a strictly homogeneous uniaxial gyrotropic medium. A small excursion in temperature might result in a variation in the magnitude of the intrinsic spontaneous magnetization, and therefore, in the values of the magneto-optical constants, but this would not involve irreversible changes in the magnetic structure, and the values of the constants would be restored on recovery of the operating temperature.

In contrast, in a material that is on or below the knee of its demagnetization curve the magnetization is far from homogeneous. A material enters the knee of its demagnetization curve when the negative field in the material approaches the intrinsic anisotropy fields in the grains. The mean magnetization in the

<sup>1</sup>The Web pages of several major suppliers of high-quality hexaferrite permanent magnet ceramics give explanatory information on these materials; in particular the TDK Corporation, Tokyo, Japan.

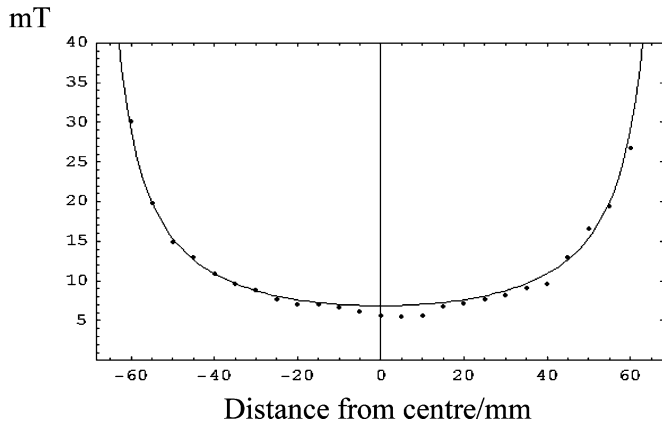


Fig. 3. Variation of the normal  $B$ -field along a diagonal on the surface of a thin square plate of FB6H heaferrite (see text).

material falls as a result of an increasing number of grains suffering reversals of their spontaneous magnetizations to take up directions close to that of the negative field. As the negative field increases further, the switched grains form thread-like clusters, or domains of reversed magnetization, which expand irreversibly to take the mean magnetization progressively and rapidly towards zero. A coherent signal beam entering a material in such an inhomogeneous magnetic state would suffer aberration or a significant loss of power due to diffuse scattering. Furthermore, variations in the ambient temperature would result in irreversible changes in the structure. A circulator having a plate in such a state would lack long-term stability.

A thin plate of a material that has been selected in accord with requirements 1) and 2) above is expected to retain near-homogeneous uniform magnetization after removal from the poling magnet. To confirm that expectation, the normal component of the  $B$ -field over the surface of the plate can be measured with a Hall-probe magnetometer. Fig. 3 illustrates a test of this type. The plotted points in Fig. 3 are measured values of the normal  $B$ -field along a diagonal on the surface of a magnetized square plate of TDK material FB6H, of thickness 2.03 mm and width 100 mm. The curve in Fig. 3 shows the field values *calculated* for a plate having a uniform magnetization of magnitude  $330 \text{ kA} \cdot \text{m}^{-1}$ , the value of the magnetization at the operating point of a plate of FB6H at  $20^\circ \text{C}$ . The field is quite weak over most of the plate's surface so the agreement in Fig. 3 between the measured and the calculated values is a sensitive confirmation of the uniformity of the magnetization in the plate following its initial poling; in fact, the measurements were made several months after the initial poling of the plate, confirming the long-term stability of the uniformly magnetized state.

### III. GYROTROPIC MAGNETOOPTICAL PROPERTIES OF CANDIDATE MATERIALS

A candidate material for use in a millimeter-wave/submillimeter-wave quasi-optical circulator must not only have the magnetostatic properties specified in Section II; it must, of course, also have the necessary gyrotropic magneto-optical properties at these frequencies, i.e., a signal beam propagating in the material along the direction of the magnetization must

suffer a Faraday rotation of its polarization at a rate of 1 rad per 1 or 2 mm of pathlength, and the attenuation of the beam must be less than  $-1 \text{ dB/mm}$ .

The high intrinsic magnetocrystalline anisotropies of the mixed-oxide hexaferrite ceramics which give these materials their good permanent magnet properties, as described in Section II, are responsible also for the strong precessional magnetic resonances that have been observed in such materials at frequencies in range of 50–60 GHz [3]; these resonances imply well-developed gyrotropic properties at higher frequencies, and our measurements on many of these materials in the range up to 170 GHz, and on some up to 450 GHz, have confirmed this expectation (Section V).

However, our measurements show that the attenuation of millimeter/submillimeter-wave signal beams in most of the commercially available hexaferrites we have tested is too high for our purposes. There are several lossy conduction processes in ionic structures as complex as those of a hexaferrite ceramic: thermally activated redistribution over lattice sites of vacancies or of ions of different valency types, vibrational motion of ions, spin-wave decay processes, and diffuse scattering at the deviations of the spontaneous magnetization from perfect homogeneity as has been discussed earlier. The chemical formulations of commercially available materials, and the several processing steps used in their preparation, have been chosen to optimize permanent magnet characteristics, without reference to their millimeter/submillimeter-wave properties. Nevertheless, for reasons that are not yet certain, a few of the commercially available hexaferrite ceramics have quite low attenuations around 100 GHz, and one or two of these also have the required magnetostatic properties set out in Section II. These materials have been used in quasi-optical circulators operating at frequencies near 90 GHz [1], [2] and in our early circulators operating at frequencies up to 280 GHz [4], [5]. However, the observed attenuations in these materials increase with frequency above 100 GHz, and we are grateful to TDK for providing samples of their material FB6H, which have been taken through supplementary processing steps which significantly reduce the attenuation at the higher frequencies of concern to us here, up to 350 GHz and beyond.

### IV. MAGNETOOPTICAL CHARACTERIZATION OF CANDIDATE MATERIALS

As explained in Section II, a fine-grained aligned hexaferrite ceramic, in a uniformly magnetized state above the knee of its demagnetization curve, in a uniform static magnetic field parallel to the magnetization, will behave magneto-optically essentially as an homogeneous uniaxial gyrotropic medium. The intrinsic symmetries of such a medium (in particular the axial-vector character of both the magnetization and the static magnetic field) determine a gyrotropic form for the RF permeability and permittivity tensors of the material and the *characteristic plane waves* propagating along the axis of such a material are circularly polarized [6]–[8]. The refractive indices and wave impedances of these characteristic plane waves are a more expedient statement of the magneto-optical properties of a material for our purposes than the permeability and permittivity tensors themselves.

The refractive index and the wave impedance for the plane wave that is circularly polarized in the clockwise sense looking along the direction of the magnetization,  $\mathbf{M}$ , will be denoted,  $n_+(\omega)$  and  $Z_+(\omega)$ , respectively, where  $\omega$  is the angular frequency of the wave; the refractive index and wave impedance for the wave having anticlockwise polarization looking along  $\mathbf{M}$  will be denoted  $n_-(\omega)$  and  $Z_-(\omega)$ . The values of  $n_+(\omega)$  and  $Z_+(\omega)$  will differ from those of  $n_-(\omega)$  and  $Z_-(\omega)$  because the wave's circular polarization has the same screw sense as  $\mathbf{M}$  in the former case and is of the opposite sense in the latter case. The values of  $n_{\pm}(\omega)$ ,  $Z_{\pm}(\omega)$  will be the same for waves propagating parallel to and antiparallel to  $\mathbf{M}$ .

A well-known simple model [6]–[8] for the dynamical response of a spontaneous magnetization,  $\mathbf{M}$ , to an applied transverse RF electromagnetic field provides an indication of how the values of  $n_{\pm}(\omega)$ ,  $Z_{\pm}(\omega)$  might be expected to vary with signal frequency  $\omega$ . The RF field induces a small transverse deviation of  $\mathbf{M}$  from the preferred axis; a restoring couple  $\mathbf{M} \times (\mathbf{H}_a - \mathbf{M})$  then acts on  $\mathbf{M}$  due to the magnetocrystalline anisotropy (which is represented here by an effective field  $\mathbf{H}_a$ ) and the demagnetizing field in the thin plate  $\mathbf{H} = -\mathbf{M}$ , and since  $\mathbf{M}$  is intrinsically associated with electronic *angular momentum* density, its response is forced *precession* with a resonance frequency  $\omega_o = \omega_a - \omega_m$  and oscillator strength  $\omega_m$ , where  $\omega_m \equiv |\gamma|M$  and  $\omega_a \equiv |\gamma|H_a$ ,  $\gamma$  being the ratio of the magnetic moment of an electron to its associated angular momentum (close in value to  $\mu_0 e/m$ , where  $e/m$  is the charge-to-mass ratio for an electron).

This precessional dynamical response directly implies the following forms for the variations with frequency of the circular-polarization refractive indices and wave impedances

$$\begin{aligned} \operatorname{Re}(n_{\pm}(\omega)) &= \sqrt{1 + \frac{\omega_m}{(\omega_a - \omega_m) \mp \omega}} \cdot \sqrt{\operatorname{Re}(\varepsilon(\omega))} \\ \operatorname{Im}(n_{\pm}(\omega)) &= \frac{1}{2} \cdot \frac{\operatorname{Im}(\varepsilon(\omega))}{\operatorname{Re}(\varepsilon(\omega))} \operatorname{Re}(n_{\pm}(\omega)) \\ \operatorname{Re}(Z_{\pm}(\omega)) &= Z_o \sqrt{1 + \frac{\omega_m}{(\omega_a - \omega_m) \mp \omega}} \cdot \frac{1}{\sqrt{\operatorname{Re}(\varepsilon(\omega))}} \\ \operatorname{Im}(Z_{\pm}(\omega)) &= -\frac{1}{2} \cdot \frac{\operatorname{Im}(\varepsilon(\omega))}{\operatorname{Re}(\varepsilon(\omega))} \operatorname{Re}(Z_{\pm}(\omega)) \end{aligned}$$

(positive square roots) where  $\varepsilon(\omega)$  is the complex transverse dielectric constant of the material.

It can be seen that  $n_+(\omega)$  and  $Z_+(\omega)$  have resonant characters, whereas  $n_-(\omega)$  and  $Z_-(\omega)$  do not, which is a consequence of the fact that free precessional motion of  $\mathbf{M}$  is of + sense.

Measurements of  $n_{\pm}(\omega)$  and  $Z_{\pm}(\omega)$  for a number of hexaferrite ceramics over the range of 50–500 GHz (Section V) confirm these general forms with values for the characteristic frequencies  $\omega_a/2\pi$  about 65 GHz and  $\omega_m/2\pi$  about 10 GHz, which are consistent with directly measured values of the strong magneto-crystalline anisotropies and with the measured magnetizations  $\mathbf{M}$  of the materials. This simple dynamical model does not include damping of the magnetic resonance, and it does not model the dielectric loss mechanisms referred to in Section III; it does not avert the need for precise measurements of the complex magneto-optical constants of candidate magnetic materials,

at the intended operational frequencies, when designing and assessing circulators (Section V).

The nonreciprocal function of a circulator is based on the phenomenon of Faraday rotation, which is due to the difference in value between  $n_+(\omega)$  and  $n_-(\omega)$ . The general character of the Faraday-rotation phenomenon can be most simply exposed by first neglecting loss processes (taking  $n_{\pm}(\omega) = \alpha_{\pm}(\omega)/(\omega/c)$  to be real) and by considering a coherent wave, which is a superposition of the two characteristic plane waves (circularly polarized,  $\pm$ ) propagating with equal complex amplitudes along the material axis, in the positive- $z$ -direction (parallel to  $\mathbf{M}$ ). In such a wave, the resultant RF  $h$ -field is

$$\begin{bmatrix} h_x \\ h_y \end{bmatrix} = \frac{1}{2} h \exp i(\alpha_+ z - \omega t) \begin{bmatrix} 1 \\ i \end{bmatrix} + \frac{1}{2} h \exp i(\alpha_- z - \omega t) \begin{bmatrix} 1 \\ -i \end{bmatrix}$$

i.e.,

$$\begin{bmatrix} h_x \\ h_y \end{bmatrix} = h \exp i(\alpha z - \omega t) \begin{bmatrix} \cos(\delta z) \\ -\sin(\delta z) \end{bmatrix}$$

where  $\alpha = (\alpha_+ + \alpha_-)/2$  and  $\delta = (\alpha_+ - \alpha_-)/2$ .

It can be seen that, over any given transverse cross section through this wave, the field is uniform and constant in direction but this direction rotates continuously with increasing  $z$  (the wave might be said to be linearly polarized, but not plane polarized). The rate of this *Faraday rotation* is  $\delta = (\alpha_+ - \alpha_-)/2$  rad per unit increment of path, and its sense is clockwise looking along  $\mathbf{M}$  when  $\alpha_- > \alpha_+$ . For a similar wave propagating in the negative  $z$ -direction, antiparallel to  $\mathbf{M}$ , the resultant RF  $h$ -field is

$$\begin{bmatrix} h_x \\ h_y \end{bmatrix} = \frac{1}{2} h \exp i(-\alpha_+ z - \omega t) \begin{bmatrix} 1 \\ i \end{bmatrix} + \frac{1}{2} h \exp i(-\alpha_- z - \omega t) \begin{bmatrix} 1 \\ -i \end{bmatrix}$$

i.e.,

$$\begin{bmatrix} h_x \\ h_y \end{bmatrix} = h \exp i(-\alpha z - \omega t) \begin{bmatrix} \cos(\delta z) \\ -\sin(\delta z) \end{bmatrix}$$

which is a Faraday rotation at the same rate, and in the *same sense looking along*  $\mathbf{M}$ , as in the case of the wave propagating parallel to  $\mathbf{M}$ . This is the nonreciprocal behavior on which circulators are based.

The frequency dependence of the rate of Faraday-rotation according to the simple dynamical model above is, thus,

$$\delta = -(\sqrt{\varepsilon(\omega)}/2c) \{ \omega_m / (1 - \omega_o^2/\omega^2) \}$$

taking  $\omega_m \ll \omega_o$ . This tends asymptotically to the value

$$\delta \Rightarrow -(\sqrt{\varepsilon}/2c)\omega_m$$

as the frequency increases. For frequencies above about 150 GHz, the rotation rate for a hexaferrite is thus nearly independent of frequency, at about 0.45 rad/mm since  $\varepsilon$  is measured to be about 20.

The lossy processes in a real material (which have been neglected in the treatment of Faraday rotation above) will result in

differing attenuations for circularly polarized plane waves of opposite sense. The Faraday-rotation effect will consequently be somewhat more complicated than indicated above. An initially linearly polarized wave would become progressively more elliptically polarized as it propagates along the axis—the Faraday-rotation then applies to the ellipse axes. Furthermore, a linearly polarized signal beam incident on a Faraday rotator will not enter the magnetized plate as a linearly polarized field because, though a quarter-wave layer of isotropic dielectric material will be bonded to each surface of the magnetized plate to improve the matching of an incident beam to the plate, the matching could not be ideal for both circularly polarized components of the beam. The performance of a circulator will deviate from the ideal for these reasons, and in order to design a circulator and assess its performance precisely, an analytical treatment of the passage of plane wave signal beams through a Faraday-rotator plate is required. The measured complex values of the magneto-optical constants of the constituent materials will be fed into this analysis. For this purpose, we introduce *ABCD optical transfer matrices* [9]–[11] for the magnetic plate and for its matching layers, as follows.

First consider the  $2 \times 2$  circular-polarization *ABCD* transfer matrices for a layer of an isotropic dielectric material  $\mathbb{T}_{\ell\pm}(\omega)$ ; these matrices relate the complex amplitudes of the circularly polarized RF electric and magnetic fields at the first of the two faces of the layer  $e_{\pm 1}, h_{\pm 1}$  to those at the second  $e_{\pm 2}, h_{\pm 2}$ ,

$$\begin{bmatrix} e_{\pm 1} \\ h_{\pm 1} \end{bmatrix} \equiv \mathbb{T}_{\ell\pm}(\omega) \begin{bmatrix} e_{\pm 2} \\ h_{\pm 2} \end{bmatrix}$$

and

$$\begin{bmatrix} e_{\pm 2} \\ h_{\pm 2} \end{bmatrix} \equiv \mathbb{T}_{\ell\pm}^{-1}(\omega) \begin{bmatrix} e_{\pm 1} \\ h_{\pm 1} \end{bmatrix}$$

where  $\mathbb{T}_{\ell\pm}^{-1}(\omega)$  is the inverse of  $\mathbb{T}_{\ell\pm}(\omega)$ . The elements of  $\mathbb{T}_{\ell\pm}(\omega)$  are determined by the optical constants of the material  $n_{\ell}(\omega)$  and  $Z_{\ell}(\omega)$ , and by the thickness of the layer  $\ell$ , thus,

$$\mathbb{T}_{\ell\pm}(\omega) = \begin{bmatrix} \cos \phi_{\ell} & \pm Z_{\ell} \sin \phi_{\ell} \\ \mp \frac{1}{Z_{\ell}} \sin \phi_{\ell} & \cos \phi_{\ell} \end{bmatrix}$$

where the complex angle  $\phi_{\ell}(\omega) \equiv (\omega/c) \cdot n_{\ell}(\omega) \cdot \ell$ . (The derivation of the *ABCD* matrices of an isotropic dielectric for linearly polarized signal beams is familiar in the literature [9], [10]; the forms above for circularly polarized beams are straightforwardly obtained from these by representing each circularly polarized beam as a superposition of linearly polarized component beams).

In the case of a plate of *uniaxial gyrotropic* material, the refractive indices and wave impedances for the two senses of circular-polarization differ; the *ABCD* matrices for a such a plate of thickness  $d$  are consequently of the following forms:

$$\mathbb{T}_{\pm d}(\omega) = \begin{bmatrix} \cos \phi_{\pm d} & \pm Z_{\pm} \sin \phi_{\pm d} \\ \mp \frac{1}{Z_{\pm}} \sin \phi_{\pm d} & \cos \phi_{\pm d} \end{bmatrix}$$

$$\mathbb{T}_{\pm d}^{-1}(\omega) = \begin{bmatrix} \cos \phi_{\pm d} & \mp Z_{\pm} \sin \phi_{\pm d} \\ \pm \frac{1}{Z_{\pm}} \sin \phi_{\pm d} & \cos \phi_{\pm d} \end{bmatrix}$$

where the complex angle  $\phi_{\pm d}(\omega) \equiv (\omega/c) \cdot n_{\pm}(\omega) \cdot d$ .

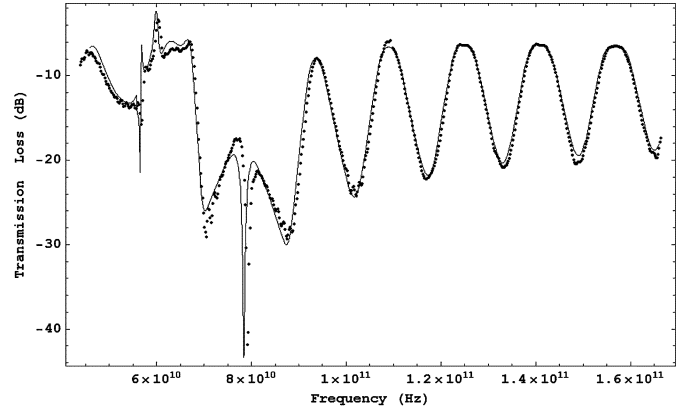


Fig. 4. Co-polar transmittance of a plate of TDK material FB6H, thickness 2.02 mm. The continuous line is the calculated transmittance and the points are measured values.

These *ABCD* matrices are used in the determination of the properties of circulators in Section VI.

## V. MEASURED VALUES OF THE MAGNETOOPTICAL CONSTANTS OF CANDIDATE MATERIALS

As noted in Section IV, it is essential, when designing and proving a high-performance circulator, to have measured values of the magneto-optical constants  $n_{\pm}(\omega)$  and  $Z_{\pm}(\omega)$ , of candidate gyrotropic materials, through the range of intended operational frequencies. We have, together with colleagues, made such measurements on a number of hexaferrites over the range from 50 to 500 GHz, using an ultra-wideband vector network analyzer and a quasi-optical test circuit containing a  $100 \times 100$  mm sample plate. The measurement method and the results obtained are to be described elsewhere [12]. We note here simply that the values of  $n_{\pm}(\omega)$  and  $Z_{\pm}(\omega)$  of a low-loss hexaferrite measured in this way accord well with the formulas in Section IV with appropriate values assigned to the parameters  $\omega_a, \omega_m$  and  $\varepsilon$ .

For example, Fig. 4 shows that the measured values of the co-polar transmittance of a 2.02-mm plate of FB6H over the range from 50 to 170 GHz (the points in Fig. 4) are closely fitted by the co-polar transmittance calculated for a 2.02-mm plate of a material having the values of  $n_{\pm}(\omega)$  and  $Z_{\pm}(\omega)$  given by the formulas in Section IV with  $\omega_a = 2\pi \times 65.9$  GHz and  $\omega_m = 2\pi \times 10.1$  GHz and  $\varepsilon(\omega) = 20.7(1 + i0.005)$  (the continuous line in Fig. 4).

## VI. DESIGN AND PERFORMANCE-VERIFICATION OF QUASI-OPTICAL CIRCULATORS.

Our current circulators are designed to admit quasi-collimated, or high-directivity, signal beams with spatial spectra of small angular-width, less than  $2^\circ$  at 100 GHz falling to  $0.6^\circ$  at 350 GHz, with further reduction as the beam passes through the Faraday-rotator plate. The analysis of the propagation of such signal beams through the circulator can, therefore, be conducted, with little error, as if for plane waves, as is illustrated in this section. Such a beam has a Gaussian beam waist of 25 mm or so at the plate, and we use a width of 100 mm for the Faraday-rotator plate to ensure negligible truncation of the beam at the edges of the plate. This scale of optical

component is acceptable for circulators that are to be incorporated in large quasi-optical measurement systems, such as those described in Section VII. However, for some applications, smaller components and beamwidths would be desirable and it is important to note that good circulator performance can be achieved with somewhat smaller optics, especially at the higher frequencies. Analysis of the propagation of a signal beam of reduced directivity, through a Faraday-rotator plate, is feasible but complicated; verification of the performance levels of such circulators comes more from test measurements than from predictive calculations. For our present purposes, we shall make plane-wave analyzes of the propagation of signal beams through circulator structures and we expect to find high-level performances that will prove to be in accord with the measured performances of circulators with 100-mm optics.

The thickness of the gyrotropic plate in a circulator  $d(\omega_s)$  is to be such that a linearly polarized signal beam at the operational frequency  $\omega_s$  would suffer a  $\pi/4$  Faraday rotation in a single pass of the plate (Section IV), i.e.,

$$d(\omega_s) = \frac{\pi/2}{\text{Re}[n_+(\omega_s) - n_-(\omega_s)] \cdot (\omega_s/c)}$$

where  $n_{\pm}(\omega_s)$  are the measured refractive indices of the material.

A quarter-wave layer of an isotropic dielectric material will be bonded to each face of the hexaferrite plate to optimize the matching of an incident linearly polarized signal beam, at operational frequency  $\omega_s$ , into the plate and out of it after a single pass of the plate. A material having a wave impedance  $Z_{\ell}(\omega_s) = 1/n_{\ell}(\omega_s)$  that is midway between the values  $\sqrt{Z_+(\omega_s)}$  and  $\sqrt{Z_-(\omega_s)}$  that would, respectively, provide ideal matching for the  $\pm$  circularly polarized components of the incident beam, is required; the match cannot be perfect since it would not be possible to match to both circularly polarized components of the incident beam ideally. The thickness of the quarter-wave layer is then

$$d_{\ell}(\omega_s) = (\pi/2)/n_{\ell}(\omega_s) \cdot (\omega_s/c).$$

The Faraday rotator is a two-port for each sense of circular-polarization independently. To analyze the passage of a signal beam through it we need to determine its  $\pm ABCD$  matrices. These are formed by multiplication of the  $\pm ABCD$  matrices of the three components [11], i.e., those of the first matching layer, of the gyrotropic plate, and of the second matching layer. The forms of the  $\pm ABCD$  matrices of these components individually have been established in Section IV with the elements of each expressed in terms of the measured thickness of the plate/layer, and of the refractive indices and wave impedances of the material of the plate/layer.

The circular-polarization reflectances and transmittances of the Faraday rotator  $r_{\pm F}$  and  $t_{\pm F}$  for each of the two senses of normal incidence are then given in terms of the elements of the rotator's  $\pm ABCD$  matrices by standard forms [11]; in turn, these are transformed into reflectances and transmittances for co- and cross-polar linear polarizations  $r_{coF}(\omega)$ ,  $r_{crF}(\omega)$  and  $t_{coF}(\omega)$ ,  $t_{crF}(\omega)$  for each direction of normal incidence, thus,

$$r_{coF}(\omega) = (r_{+F}(\omega) + r_{-F}(\omega))/2$$

$$r_{crF}(\omega) = i(r_{+F}(\omega) - r_{-F}(\omega))/2$$

$$t_{coF}(\omega) = (t_{+F}(\omega) + t_{-F}(\omega))/2$$

$$t_{crF}(\omega) = i(t_{+F}(\omega) - t_{-F}(\omega))/2.$$

These several reflectances and transmittances of the rotator are the elements of the circulator's scattering matrix [11] [assuming the wire grids in the circulator to be ideal in performance (see Section VII)]. The scattering matrix of an *ideal* four-port circulator that gives signal-power transfers between the four ports according to the scheme  $1 \Rightarrow 2, 2 \Rightarrow 3, 3 \Rightarrow 4$  and  $4 \Rightarrow 1$  is

$$\begin{bmatrix} S_{11} & S_{12} & S_{13} & S_{14} \\ S_{21} & S_{22} & S_{23} & S_{24} \\ S_{31} & S_{32} & S_{33} & S_{34} \\ S_{41} & S_{42} & S_{43} & S_{44} \end{bmatrix} = \begin{bmatrix} 0 & 0 & 0 & 1 \\ 1 & 0 & 0 & 0 \\ 0 & 1 & 0 & 0 \\ 0 & 0 & 1 & 0 \end{bmatrix}$$

where 1 here indicates unit modulus with arbitrary phase. The elements in the scattering matrix of a real circulator will deviate (a little) from these ideal values, 0 or 1, as a result of the difference in attenuation between the two senses of circular polarization in the hexaferrite, and of the imperfect matching of an incident linearly polarized beam into the magnetized plate. The sequence of calculations outlined above starts with the measured values of the thicknesses of the three components of the rotator and with the measured complex magneto-optical constants of the materials in these components, and traces the effects of the nonidealities through to the values of the elements in the circulator's scattering matrix. The performance of a circulator is usually stated in terms of the values in decibels of the following parameters:

- insertion loss  $L \equiv 1 - |S_{21}|^2$ ;
- isolation  $I \equiv |S_{21}|^2/|S_{12}|^2 \simeq |S_{12}|^{-2}$ ;
- back reflectance  $R \equiv |S_{11}|^2$ .

We use this sequence of calculations, written into a Mathematica [13] worksheet, to predict levels of performance to be expected of particular circulators. Some illustrative examples are given below.

The curves in Figs. 5 and 6 show the predicted performances of a 100-GHz circulator based on TDK hexaferrite FB6H in the magnetized plate and, for the matching layers, a loaded polymer having a refractive index close to the optimum value for matching to FB6H at 100 GHz.

A circulator to this design was manufactured and its performances were measured; the points in Figs. 5 and 6 show the results of the measurements. The close agreement between the predicted and measured values of the isolation in Fig. 5 and of the insertion loss in Fig. 6 confirms the reliability of our design and assessment procedures and of our manufacturing methods (Section VII).

The isolation obtained with this circulator near 100 GHz ( $-46$  dB), and the insertion loss ( $-0.35$  dB), would suffice for many demanding applications. If yet better values of isolation were required, it would be possible to use two such circulators in series, at the expense of a doubling of the insertion loss.

If the back reflectance at 100 GHz, about  $-25$  dB, were not sufficiently low for a particular application, there is a very simple remedy: set the Faraday rotator at a small angle off-set from normal incidence to de-couple the incident and returned

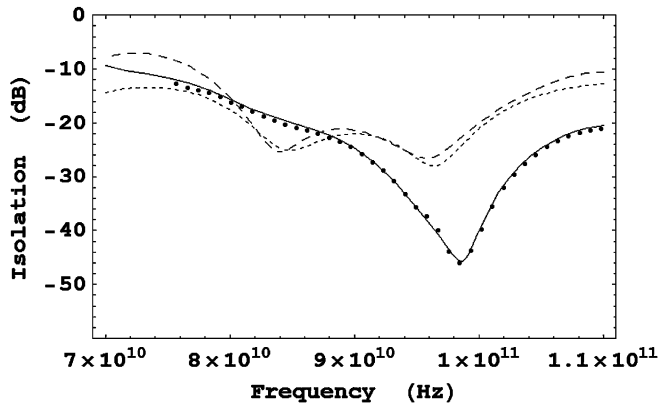


Fig. 5. Predicted isolation (continuous line) and back reflectances (co-polar: long dashed line; cross-polar: short dashed line) for a circulator designed to give optimum performance at 100 GHz. The points are measured isolations.

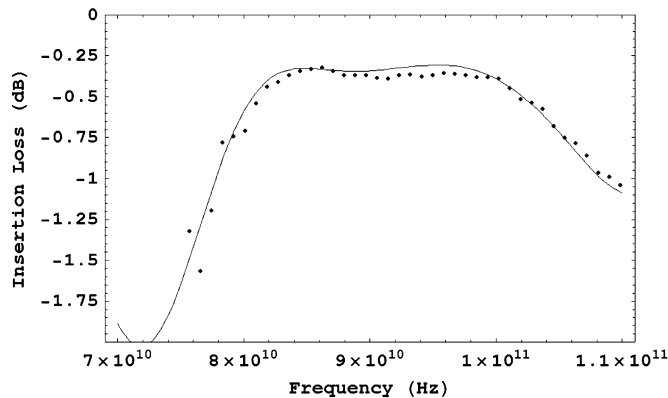


Fig. 6. Predicted insertion loss (line) for a circulator designed to give optimum performance at 100 GHz. The points are measured insertion losses.

signal beams. The high directivity of the signal beams at the Faraday rotator means that an angle of incidence of no more than a degree or two will efficiently decouple the incident and returning beams and an offset as small as this results in a negligible change in isolation performance. (Useful performance levels can in fact be obtained with a Faraday rotator set at quite a large angle of incidence [14].)

The 10% bandwidth (for isolations better than  $-30$  dB) of this circulator is determined by the dispersion of the Faraday-rotation rate in the region of 100 GHz (Section IV).

Similar circulator performances at 90 GHz have recently been reported by colleagues [2]. The research reported in this paper has been directed to achieving comparable performance levels in circulators operating at higher frequencies, up to 300 GHz and beyond. Figs. 7 and 8 show the predicted and measured performances of a circulator designed to give optimum isolation at 240 GHz and they illustrate the extent to which we have succeeded in this.

This 240-GHz circulator uses modified TDK hexaferrite FB6H for the magnetized plate and, for the matching layers, a loaded polymer having a refractive index close to the optimum value for matching to FB9H at 240 GHz. The measured values of the magneto-optical/optical constants of these materials (Section V) served to determine (through the expressions above) values for the design thicknesses of the plate and of

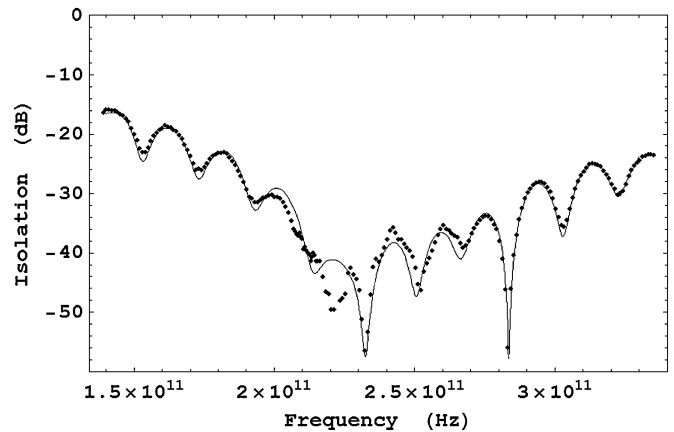


Fig. 7. Isolation of a circulator designed for optimum performance at 240 GHz. The line is the predicted performance and the points are the measured values.

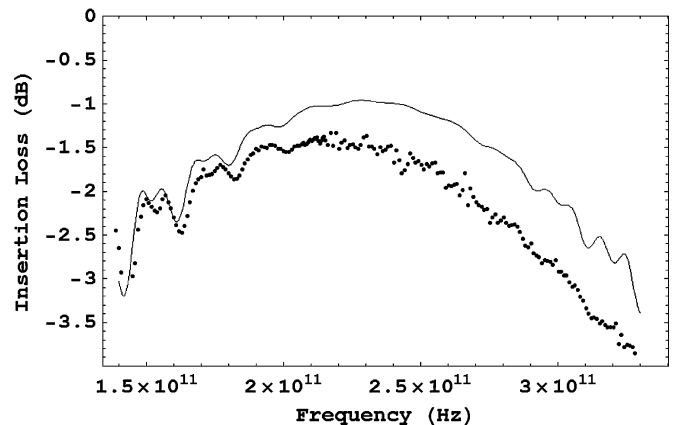


Fig. 8. Insertion loss of a circulator designed for optimum isolation at 240 GHz. The thin line is the predicted performances and the points are the measured values.

the matching layers. The values of these thicknesses as gauged after manufacture are close to the design values and are used in the calculating the predicted performances shown in these figures.

The values of isolation (better than  $-40$  dB) and of insertion loss (better than  $-1.6$  dB) provided by this circulator at 240 GHz are comparable with those obtained at 100 GHz. The 30% bandwidth (at better than  $-30$  dB) is much greater than that of the 100-GHz circulator, however, which is a consequence of the fact that the dispersion of the Faraday-rotation rate is much less at this higher frequency than at the lower frequency (Section IV).

The very wide bandwidth reveals oscillatory features in the curves of Fig. 7 due to standing waves in the ferrite plate attributable to the decreasing efficiency of the matching layers away from the 240-GHz design frequency.

Prediction calculations can be used to assess the dimensional tolerances on the components of a Faraday rotator. For example, Fig. 9 shows the predicted isolation of a circulator at the design operational frequency, 240 GHz, as a function of the thickness of the matching layer and of the relative permittivity of the material of the layer. The surface in Fig. 9 is truncated at  $-40$ -dB isolation in order to make clear the tolerances on the values of the thickness and refractive index of the matching layer required

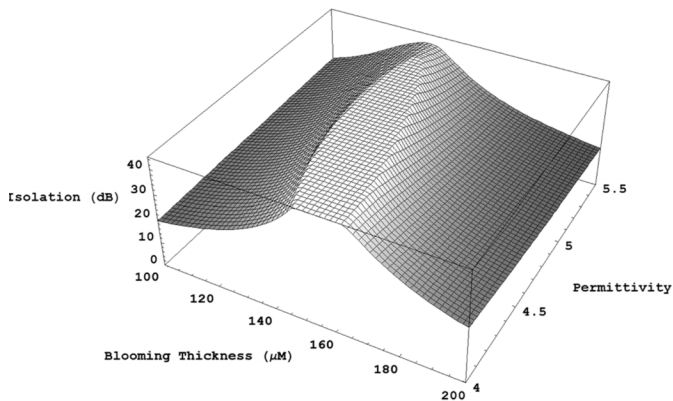


Fig. 9. Predicted isolation of a circulator at 240 GHz as a function of the thickness of the matching (or blooming) layers (in micrometers), and of the relative permittivity of the material of the layer.

to assure an isolation at that level or better. The tolerance on the thickness is quite tight, less than  $\pm 10 \mu\text{m}$  in  $145 \mu\text{m}$ . The tolerance on the relative permittivity is about  $\pm 0.25$  in 4.8 (a tolerance that can be met with loaded-polymer materials).

The illustrations in this section demonstrate the reliability both of our prediction procedures and of our manufacturing methods for circulators over the range 100 to 350 GHz.

## VII. MANUFACTURE AND APPLICATIONS OF QUASI-OPTICAL CIRCULATORS.

The manufacture of a quasi-optical circulator involves a number of fabrication processes carried through at high precisions. Specialist toolmaking expertise is required for this. The circulators we have tested (Section VI), and those we have provided for installation in major measurement systems, as described below, were manufactured by Thomas Keating Ltd., Billingshurst, West Sussex U.K.

To fabricate the Faraday rotator a 100-mm square sheet of a selected hexaferrite ceramic is ground to flatness and specified thickness. A layer of a selected loaded-polymer is then thermally bonded to one face of the ferrite plate and is ground to specified thickness; and the process is repeated for the second face. In grinding these difficult materials to  $10\text{-}\mu\text{m}$  tolerances or tighter there must be careful control to avoid distortions.

The composite Faraday-rotator plate is then magnetized to saturation in the close-fitting pole gap of a high-field electromagnet, and is removed progressively from the magnet, in a controlled reduction of the poling field, to leave the plate uniformly and stably magnetized.

The wire grids of the circulator are wound on 100-mm frames ground flat to  $10 \mu\text{m}$ , with wire of  $10\text{-}\mu\text{m}$  diameter, at a  $25 \pm 3\text{-}\mu\text{m}$  spacing. Such grids show cross-polar leakage at the  $-50\text{-dB}$  level in the 100–300-GHz range [15].

The planar power dumps required in the circulator/isolator are injection-moulded pyramidal-arrays of carbon-loaded polymer with needle-sharp points to the pyramids. They have monostatic reflectances less than  $-40 \text{ dB}$  [16].

Scalar feed-horns and collimating reflectors will usually be required in a circulator unit, which can be designed to be very wideband and manufactured in a modular configuration.

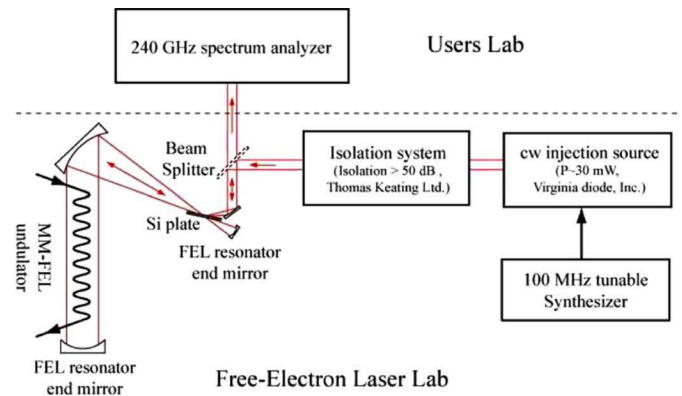


Fig. 10. Schematic of the UCSB FEL injection-locked at 240 GHz [17].

We cite below several major measurement systems the successful operation of which has depended on the circulators/isolators of this type that we have provided.

### A. Dual-Frequency Interferometers to Measure Electron Densities in Fusion Plasmas

The electron densities in large fusion-plasma machines are measured by millimeter-wave interferometry. Dual-frequency (two-color) interferometers are required for this in order to distinguish between the effects of the changing electron-density during the pulsed operation of the plasma, and those of the concomitant changes in the path length through the long transmission lines to and from the plasma (up to 100 m through biological shields). The appropriate frequencies for such measurements are in the range from 100 to 300 GHz. We have provided the complex quasi-optical circuits for two such systems which include several high-performance circulators or isolators to assure the required dynamic ranges and phase-lock stabilities [4], [5]. The first of these systems (operating at 130 and 200 GHz) was installed on the Joint European Torus (JET), Abingdon, UK. The second (at 140 and 280 GHz) was for the large helical device (LHD) at the National Institute for Fusion Science, Nagoya, Japan, and this is currently operating efficiently almost a decade after first installation, testifying in particular to the long-term stability of its six isolators.

### B. Free Electron Laser (FEL) Injection Locked at 240 GHz

The FEL at the University of California at Santa Barbara (UCSB) provides high-power microsecond pulses, tunable from 120 to 890 GHz, for application in a wide range of measurement sciences.<sup>2</sup> The free-running FEL generates power simultaneously in many longitudinal cavity modes, separated in frequency by 25 MHz, with pulse to pulse variations. The FEL can, however, be locked into a single selected cavity mode by injecting a few milliwatts of coherent power, at the frequency of the selected mode, from a tunable solid-state-diode source. A circulator/isolator must be inserted between the FEL and diode, as illustrated in Fig. 10, to protect the diode from the high power issuing from the FEL.

<sup>2</sup>The UCSB Center for Terahertz Science and Technology FELs. [Online]. Available: <http://sbfel3.ucsb.edu>

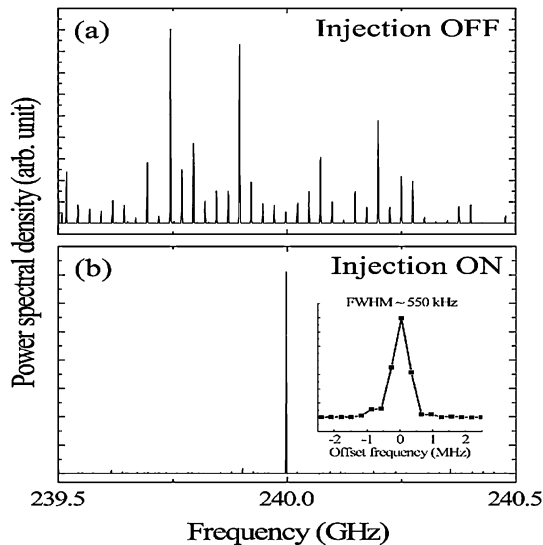


Fig. 11. (a) Multimode structure of a 240-GHz pulse from the UCSB FEL with no injection-locking signal. (b) Single high-power line obtained with injection locking (the insert shows the extremely narrow width of this line). Reprinted, with permission, from [17].

We provided isolators for injection-locking at 240 GHz. The specified isolation was  $-50$  dB or better to provide adequate protection of the diode. In order to assure this long-term, two circulators like the one described in Section VI were connected in series, with the Faraday rotators offset by a few degrees from normal incidence to eliminate back reflectance.

The successful phase locking of the FEL at 240 GHz is illustrated in Fig. 11 [17]. The spectrum of a multimode output pulse from the FEL, when free running at a nominal 240 GHz, is shown in Fig. 11(a). When the injection-locking is switched on, the spectrum of the output becomes a single very narrow high-power line at 240 GHz, as shown in Fig. 11(b)

Such single-mode operation will be crucial for many future applications of the FEL including high-power high-frequency pulsed electron-spin-resonance studies in molecular biology [18].

It should be noted that the wide bandwidth of the circulator (Section VI) means that (given appropriate solid-state diode sources) the FEL could be injection locked at any mode frequency in a 30% band; and, since the quasi-optical circuit is extremely wideband, it would be a simple matter to replace the Faraday-rotator plates by others to achieve locking at any specified frequency in the range from 120 to 400 GHz.

### C. Measurement of the Millimeter/Submillimeter-Wave Antenna Patterns of a Spaceborne Instrument for Studying the Cosmic-Background Radiation

PLANCK is a European Space Agency (ESA) mission to study the millimeter/submillimeter-wave cosmic background

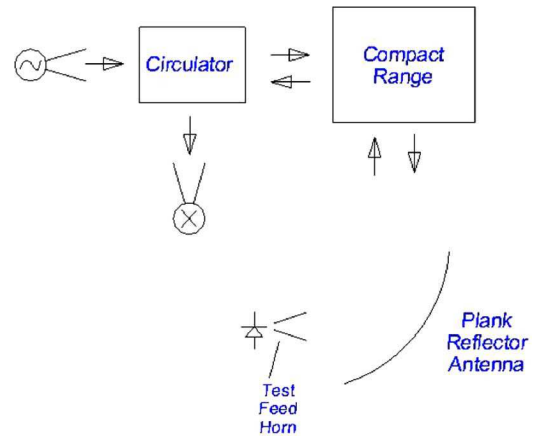


Fig. 12. Schematic of the configuration for the measurement of the 320-GHz monostatic radar cross section of the Planck HFI. The test feed horn is one of many in the focal plane array.

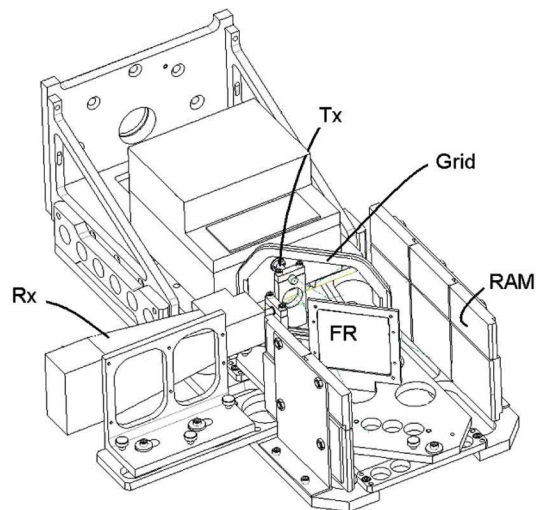


Fig. 13. Feed-module for the compact range (see text).

radiation<sup>3</sup> and is due for launch in the coming year. The flight model of the high-frequency instrument (HFI) on PLANCK has been under test in the large antenna test range at Alcatel, Cannes, France, to verify the antenna patterns, and to check the alignment of the focal-plane feed-horn array. These tests required the measurement of the 320-GHz monostatic radar cross section of the HFI as the instrument, together with the reflector antenna, was rotated on the turntable of the antenna range [19]. The test configuration is shown schematically in Fig. 12; the 320-GHz circulator that separates the returning beam from the outgoing beam is a crucial component.

We provided the feed-module depicted in Fig. 13, which incorporates the circulator and feed horns, and housings for the source and receiver. It was important to divert any signal power back reflected from the Faraday-rotator plate from the receiver feed horn so the Faraday plate was offset from normal incidence. The diverging outgoing beam, and the converging

<sup>3</sup>The Planck Mission. [Online]. Available: [http://www.esa.int/esaSC/120398\\_index\\_0\\_m.html](http://www.esa.int/esaSC/120398_index_0_m.html)

returning beam, passed through the circulator plate with little aberration with a two-way insertion loss of  $-4$  dB.

The qualification tests of HFI were successfully undertaken with this system [20].

### VIII. CONCLUDING SUMMARY

The objective of this study was to establish procedures for the design, manufacture, and verification of wideband high-performance circulators/isolators operating at frequencies beyond 100 GHz, that is to say, above the frequencies for which high circulator performances have previously been demonstrated [2]. Electromagnetic waves in the range from 100 to 350 GHz and beyond are finding major applications in astronomy and cosmology, in climatology, meteorology, and atmospheric science, in the diagnostics and heating of thermonuclear plasmas, in spectroscopic studies of materials, nanostructures, and biomolecules, and in high-resolution radar; applications in communications systems are under development. There will be many opportunities for system designers to make use of the special signal-control functions afforded by high-performance wideband circulators once the feasibility of such components at these frequencies is recognized. The purpose of this paper has been to further that recognition.

### ACKNOWLEDGMENT

The authors wish to thank P. Goy for measurements made with the AB-Millimetre vector network analyzer (Figs. 4, 7, and 8), S. Begley, Agilent Technologies, for measurements on the 100-GHz circulator (Figs. 5 and 6), M. Shewin, J. Ramian, and S. Takahashi for permission to use Figs. 10 and 12, M. Paquay and M. van der Vorst for information on the Planck HFI tests, and especially H. Taguchi and K. Suzuki, both with the TDK Corporation, for supplying modified versions of one of their standard ferrite products.

### REFERENCES

- [1] R. J. Wylde, "Gaussian beam-mode circuits for millimetre wave-lengths," Ph.D. dissertation, Phys. Dept., Queen Mary College, Univ. London, London, U.K., 1992.
- [2] R. I. Hunter, D. A. Robertson, P. Goy, and G. M. Smith, "Design of high performance millimeter wave and sub-millimeter wave quasi-optical isolators and circulators," *IEEE Trans. Microw. Theory Tech.*, vol. 55, no. 5, pp. 890–898, May 2007.
- [3] K. N. Kocharyan, M. N. Afsar, and I. I. Tkachov, "New method for measurements of complex magnetic permeability in the millimeter-wave range—Part II: Hexaferrites," *IEEE Trans. Magn.*, vol. 35, no. 4, pp. 2104–2110, Jul. 1999.
- [4] K. Kawahata, K. Tanaka, Y. Ito, A. Ejiri, and R. J. Wylde, "A two-color millimetre-wave interferometer for the measurements of line integral electron density on large helical device," *Rev. Sci. Instrum.*, vol. 70, no. 1, pp. 695–698, Jan. 1999.
- [5] R. Prentice, T. Edlington, R. T. C. Smith, D. L. Trotman, R. J. Wylde, and P. Zimmerman, "A two-color mm-wave interferometer for the JET divertor," *Rev. Sci. Instrum.*, vol. 66, no. 2, pp. 1154–1158, Feb. 1995.
- [6] P. J. B. Clarricoats, *Microwave Ferrites*. London, U.K.: Chapman & Hall, 1961.

- [7] K. J. Standley, *Oxide Magnetic Materials*. Oxford, U.K.: Clarendon, 1972.
- [8] A. J. Baden-Fuller, *Ferrites at Microwave Frequencies*. London, U.K.: IEE, 1987.
- [9] M. Born and E. Wolf, *Principles of Optics*. New York: Pergamon, 1980.
- [10] G. R. Fowles, *Introduction to Modern Optics*. New York: Holt, Rinehart and Winston, 1968.
- [11] D. M. Pozar, *Microwave Engineering*. New York: Wiley, 1998.
- [12] B. Yang, P. Goy, D. H. Martin, R. J. Wylde, and R. Donnan, "Measurement of the optical and magneto-optical constants of materials from 50 GHz to 500 GHz," unpublished.
- [13] S. Wolfram, *Mathematica 5*. Champaign, IL: Wolfram Res. Inc., 2004.
- [14] B. Lax, J. A. Weiss, N. W. Harris, and G. F. Dionne, "Quasi-optical ferrite reflection circulator," *IEE Trans. Microw. Theory Tech.*, vol. 41, no. 12, pp. 2190–2197, Dec. 1993.
- [15] T. Manabe, J. Inatani, A. Murk, R. J. Wylde, M. Seta, and D. H. Martin, "A new configuration of polarization-rotating dual-beam interferometer for space use," *IEEE Trans. Microw. Theory Tech.*, vol. 51, no. 6, pp. 1696–1704, Jun. 2003.
- [16] A. Lonnqvist, A. Tamminen, J. Mallat, and A. V. Raisanen, "Monostatic reflectivity measurements of radar absorbing materials at 310 GHz," *IEEE Trans. Microw. Theory Tech.*, vol. 54, no. 9, pp. 3491–3486, Sep. 2006.
- [17] S. Takahashi, G. Ramian, M. S. Sherwin, L.-C. Brunel, and J. van Tol, "Sub-MHz linewidth at 240 GHz from an injection-locked free-electron laser," 2007. [Online]. Available: <http://xxx.lanl.gov/abs/0706.1116>, arXiv:0706.1116v1 [cond-mat.other]
- [18] P. C. Riedi and G. M. Smith, "Progress in high field ESR," in *Electron Paramagnetic Resonance*. London, U.K.: Roy. Soc. Chem., 2002, vol. 18, ch. 9, sec. 3.
- [19] R. Hills, Jan. 2005, Cambridge Univ., Cambridge, U.K., private communication.
- [20] M. Paquay, J. Marti-Canales, L. Rolo, G. Forma, D. Dubruel, R. Wylde, B. Maffei, D. Doyle, G. Crone, J. Tauber, and R. Hills, "Alignment verification of the PLANCK reflector configuration by RCS measurements at 320 GHz," presented at the EuMW, 2008.



**Derek H. Martin** received the B.Sc. and Ph.D. degrees in physics from the University of Nottingham, Nottingham, U.K., in 1950 and 1954, respectively.

Since then, he has been with Queen Mary College, University of London, London, U.K., where he is an Emeritus Professor of physics and an Honorary Fellow. He was Editor of *Advances in Physics* (1973–1983). His research interests have included experimental studies of collective excitations in solids, of the Earth's atmosphere and of the cosmic microwave background, and in thermonuclear

plasma diagnostics, all using terahertz electromagnetic waves.

Dr. Martin is a Fellow of the Institute of Physics, of which he served as honorary secretary (1984–1994). He was the recipient of the 1983 Metrology Award of the U.K. National Physical Laboratory, and the 1992 SPIE Kenneth J. Button Prize for his inception of polarization interferometry.



**Richard J. Wylde** received the B.A. degree in natural sciences from Sidney Sussex College, Cambridge, U.K., in 1979, and the Ph.D. degree in physics from Queen Mary College, University of London, London, U.K., in 1985.

He is currently an Honorary Reader with the School of Physics and Astronomy, University of St. Andrews, Fife, U.K. He also manages Thomas Keating Ltd., Billingshurst, West Sussex, U.K., and QMC Instruments Ltd. His research interests include the design of terahertz systems for use

in thermonuclear plasma diagnostics, observational cosmology, astronomy, electron-spin-resonance spectroscopy, and atmospheric remote sensing.

Dr. Wylde is a Fellow of the Institution of Engineering and Technology.